

# RSC Advances



This is an *Accepted Manuscript*, which has been through the Royal Society of Chemistry peer review process and has been accepted for publication.

*Accepted Manuscripts* are published online shortly after acceptance, before technical editing, formatting and proof reading. Using this free service, authors can make their results available to the community, in citable form, before we publish the edited article. This *Accepted Manuscript* will be replaced by the edited, formatted and paginated article as soon as this is available.

You can find more information about *Accepted Manuscripts* in the [Information for Authors](#).

Please note that technical editing may introduce minor changes to the text and/or graphics, which may alter content. The journal's standard [Terms & Conditions](#) and the [Ethical guidelines](#) still apply. In no event shall the Royal Society of Chemistry be held responsible for any errors or omissions in this *Accepted Manuscript* or any consequences arising from the use of any information it contains.



## ARTICLE

## High performance NiO microsphere anode assembled from porous nanosheets for lithium-ion batteries

Lihua Chu<sup>a</sup>, Meicheng Li<sup>\*ab</sup>, Xiaodan Li<sup>a</sup>, Yu Wang<sup>a</sup>, Zipei Wan<sup>a</sup>, Shangyi Dou<sup>a</sup>, Dandan Song<sup>a</sup>, Yingfeng Li<sup>a</sup> and Bing Jiang<sup>a</sup>

Received 00th March 2015,  
Accepted 00th January 20xx

DOI: 10.1039/x0xx00000x

www.rsc.org/

3D NiO microspheres assembled from porous nanosheets are prepared and evaluated as anode material for lithium ion battery, showing excellent electrochemical performance with high lithium storage capacity, satisfactory cyclability and rate performance. The NiO microspheres deliver a first discharge capacity of 1242 mA h g<sup>-1</sup> and remain a reversible capacity up to 820 mA h g<sup>-1</sup> after 100 cycles at a current of 100 mA g<sup>-1</sup> in half cell. And it exhibits ameliorative rate capacity of 634 mA h g<sup>-1</sup> at the current of 1 A g<sup>-1</sup>. The high lithium-storage performance can be mainly ascribed to the porous nanosheets, which improve lithium ions transfer, provide sufficient electrode/electrolyte contact areas and better accommodation of volume change with the lithiation/delithiation process. Moreover, the 3D microsphere architecture are also helpful for enhancing the electrochemical performance of the lithium ion battery. The results indicate the great potential of the 3D NiO microspheres assembled from porous nanosheets used as the anode materials for lithium ion batteries.

### Introduction

With the rapid development of the global economy, the fast depletion of non-renewable energy, and the increasing environmental problems, it is urgent to develop new clean and sustainable sources of energy and new technology of energy storage and energy conversion with high efficiency.<sup>1-3</sup> Rechargeable lithium-ion batteries (LIBs) are one promising energy storage and conversion technology for the upcoming high demand such as electric vehicles and grid storage systems because of their high energy density, long life-span, no memory effect and environmental benignancy.<sup>4</sup> Whereas, the commercial used graphite anode materials with low specific capacity (theoretical capacity is 372 mA h g<sup>-1</sup>) and low lithium ion mobility are not sufficient to meet the demands of modern development. Hence, alternative anode materials with higher capacities are urgently needed to increase the energy density and performance of lithium-ion batteries.

A series of transition metal oxide has been exploited for anode materials in LIBs.<sup>5-7</sup> Among of these, NiO have drawn attention because of their high theoretical capacity (717 mA h g<sup>-1</sup>), high abundance, non-toxicity, environmental benignity and low cost. However, the practical utilization of NiO is still low owing to its poor rate performances and insufficient cycling due to the poor conductivity and volume change and subsequently particle pulverization upon lithiation/delithiation.<sup>8</sup> Therefore, it is crucial to increase the

lithium ion mobility, mitigate the pulverization, and further enhanced the structural stability. To date, several strategies have been undertaken to enhance the performance of the NiO electrode materials. One well-established method relies on the design and synthesis nanostructured materials such as microspheres,<sup>9</sup> nanosheets,<sup>10</sup> three dimensional (3D) flower-like hierarchical architectures,<sup>11</sup> nanotubes,<sup>12</sup> expecting to promote the electrochemical performance and maintain the good structural integration. The most popular among various kinds of nanostructured electrode materials are porous ones, which provide the structural flexibility for volume change and the routes for fast Li<sup>+</sup> diffusion leading to enhanced performance.<sup>4-6</sup> Therefore, in consideration of the strategy mentioned above, constructing porous nano architecture is meaningful to enhance the electrochemical performance of LIBs.

Herein, we design a kind of 3D NiO microspheres architecture assembled from porous nanosheets as excellent anode materials in lithium-ion batteries. The advantageous of the combination of the porous nanosheets and 3D architecture endows the as prepared 3D NiO microspheres a good performance of stable and high reversible discharge capacity up to 820 mA h g<sup>-1</sup> even after 100 cycles at a current density of 100 mA g<sup>-1</sup>, and a good rate capability of 634 mA h g<sup>-1</sup> at a high current density of 1 A g<sup>-1</sup>, which open up new opportunities in the development of high performance LIBs.

### Experimental

#### Synthesis of 3D NiO microspheres

The 3D NiO microspheres were prepared by precipitation and a hydrothermal process. All reagents used in the experiments

<sup>a</sup> State Key Laboratory of Alternate Electrical Power System with Renewable Energy Sources, North China Electric Power University, Beijing, 102206, China. E-mail: mcli@ncepu.edu.cn; Fax: +86 10 6177 2951; Tel: +86 10 6177 2951

<sup>b</sup> Chongqing Materials Research Institute, Chongqing 400707, China

were in analytical grade and used without further purification. Distilled water was used for all synthesis and treatment processes. The preparation of Ni(OH)<sub>2</sub> was performed as follows. Typically, 0.7134 g of Ni(NO<sub>3</sub>)<sub>2</sub>·6H<sub>2</sub>O and 0.25 g of polyvinyl pyrrolidone K30 (PVP-K30) were dissolved in 40 mL of distilled water, adjusting the pH to 10.9 with ammonia, using a pH meter and magnetic stirrer to form a homogeneous solution at room temperature. The solution was then transferred into a Teflon-lined stainless steel autoclave (50 mL), sealed, and heated at 150 °C for 15 h. The greenish product was collected by centrifugation, washed with deionized water and ethanol several times to remove impurity, and then dried at 60 °C in vacuum. Finally, the NiO nanostructures were obtained by heating the hydroxide precursor at 600 °C for 2 h in air.

### Material Characterization

The morphology of the as synthesized NiO products was observed by FEI Quanta 200F microscope field emission scanning electron microscope (FESEM) and Tecnai G2 F20 field emission transmission electron microscopy (TEM) with accelerating voltage of 200 kV. The crystalline phase was identified by a Bruker D8 Focus X-ray powder diffractometer with using Cu K<sub>α</sub> (λ=1.5406 Å) radiation over a range of 2θ from 20° to 90°. The thermogravimetric/differential thermal analysis (TG/DTA) measurement was performed using STA6000 thermogravimetric analyzer in air at a scan rate of 10 °C/min from room temperature to 600 °C. Brunauer-Emmett-Teller (BET) surface areas of the samples were analyzed by nitrogen adsorption-desorption measurement on a Quantachrome Autosorb-IQ-MP sorption analyzer with prior degassing under vacuum at 77K. Pore size distribution was derived from desorption branch by a Barrett Joyner Halenda (BJH) method.

### Electrochemical measurement

The working electrodes were fabricated by coating a slurry containing 80 wt% of 3D NiO microspheres, 10 wt% of acetylene black (Super-P), and 10 wt% of polyimide dissolved in N-methyl-2-pyrrolidinone onto a copper foil and dried at 300 °C in vacuum for 2 h before pressing. Standard CR2032-type coin cells were assembled in an Ar-filled glove box (KIYON, Korea) by using the as-prepared anode, Li metal foil (0.4 mm thick) as the counter electrode, and a separator (Solupor 7P03A). The electrolyte was 1 M LiPF<sub>6</sub> dissolved in a mixture of ethylene carbonate (EC) and dimethyl carbonate (DMC) (v/v = 1:1). The cells were aged for 12 h before the measurements. Galvanostatic discharge-charge (GDC) experiments were performed at different current densities in the voltage range of 0.01–3.00 V with a multichannel battery tester (Maccor, Inc, USA). Cyclic voltammetry (CV) measurements were conducted by the electrochemical workstation (Solartron Potentiostat and Impedance Analyser, UK). Electrochemical impedance spectra (EIS) were measured using the same electrochemical workstation by applying an AC voltage of 10 mV amplitude over the frequency range from 100 kHz to 100 mHz.

## Results and discussion

The prepared NiO product shows excellent crystallinity as evidenced by powder X ray diffraction (XRD). The XRD spectra are shown in Fig. 1. All the diffraction peaks observed can be perfectly indexed to the pure NiO products with face centred cubic phase (JCPDS No 47-1049, space group Fm3m). The diffraction peaks, at 37.24°, 43.27°, 62.87°, 75.41° and 79.41°, correspond to the (111), (200), (220), (311) and (222) planes, respectively. The sharp diffraction peaks reflect the excellent crystallinity of NiO. Moreover, no other peaks arising from impurities can be observed, indicating the pure phase of as prepared NiO product.

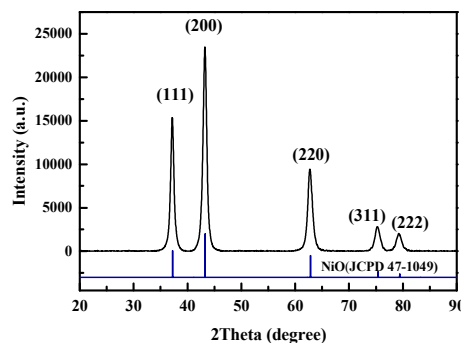


Fig. 1 X ray diffraction pattern of 3D porous nanosheets-assembled NiO microspheres obtained at room temperature as well as the standard JCPD card of NiO

The morphology and architecture of as prepared NiO product was visualized by scanning electron microscopy (SEM) and transmission electron microscopy (TEM). The corresponding images are shown in Fig. 2. From the low-magnification FESEM image (Fig. 2(a)), it can be observed that the product shows uniform 3D microsphere architecture. The high-magnification image (Fig. 2(b)) clearly shows that the microsphere have a size of 2-3 μm and are assembled porous nanosheets. The TEM image (Fig. 2(d)) further depicts that the nanosheets are porous,<sup>7</sup> with the pore diameter about 5 nm, which could facilitate lithium ions migration and buffer the volume change during the lithiation/delithiation process.<sup>8, 9</sup> The formation of the pores should be credited to the decomposition of Ni(OH)<sub>2</sub> precursors and the high reaction/etching rate at the defect sites in the precursor nanosheets during calcination. The high resolution TEM (HRTEM) image of the 3D NiO microspheres and its corresponding fast Fourier transform (FFT) pattern are shown in Fig. 2(e-f). The interplanar spacing of 2.4 Å and 1.5 Å of the resolved lattice fringes consistent with the (111) and (220) planes of the NiO crystal, respectively.

The thermal decomposition behavior of as synthesized Ni(OH)<sub>2</sub> precursor was evaluated to study the conversion process, by TG/DTA measurement. The endothermic peak at 314 °C in the derivative weight curve can be observed, as shown in Fig. 3. The weight loss of 22% are attributed to the solvent evaporation and thermal decomposition of Ni(OH)<sub>2</sub> to

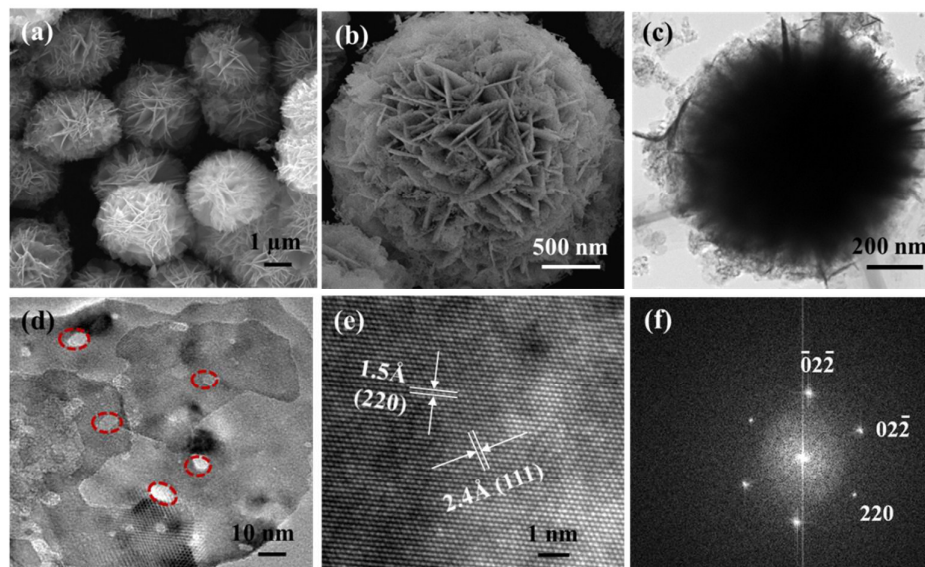


Fig. 2 (a) low- and (b) high-magnification SEM images of the porous nanosheets-assembled NiO microspheres (c)-(d) TEM images and (e) HRTEM image of the porous nanosheets-assembled NiO microspheres

NiO. The observed weight loss is close to the calculated loss value of 19.4%. No weight loss could be observed above 550 °C. Thus, it is concluded that the  $\text{Ni}(\text{OH})_2$  precursor can decompose to form NiO at above 314 °C. The calcining temperature was 600 °C in our experiment, and thus pure NiO phase was obtained.

NiO are uniform with a narrow pore size distribution. And the mesoporous volume is  $0.64 \text{ cm}^3/\text{g}$ . The pores at about 61 nm are related to the interspace between NiO nanosheets. Moreover, the surface area is about  $83.97 \text{ m}^2/\text{g}$ , which is similar with the value of mesoporous NiO.<sup>8, 11</sup>

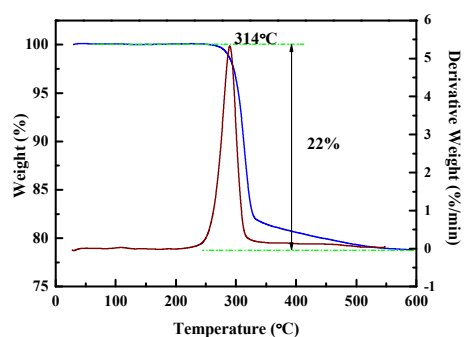


Fig. 3 TG/DTA curves of the porous nanosheets-assembled NiO microspheres

To further present specific textural properties of as prepared NiO microspheres, the specific surface area was characterized by BET nitrogen adsorption-desorption analysis, as shown in Fig. 4. In terms of shape, the adsorption isotherm can be classified as type IV curves with a type III hysteresis loops, which is indicating the existence of slit-shaped pores, according to the IUPAC classification. A distinct hysteresis loop can be observed in the large range of ca 0-0.98  $P/P_0$ , indicating the existence of mesopores and macropores.<sup>10</sup> The BJH pore size distribution calculated from the adsorption branch is presented as the inset in Fig. 4. The first peak at the mean value of 4.3 nm is due to mesoporous channels, which is consistent with the result of TEM, indicating that the pores of

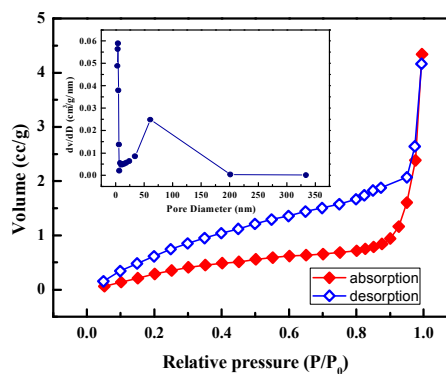


Fig. 4 Nitrogen adsorption-desorption isotherms of the porous nanosheets-assembled NiO obtained by hydrothermal synthesis.

Lithium storage properties of as prepared 3D NiO microspheres assembled porous nanosheets were investigated by CV and discharge-charge measurements in half cell configuration. The CV curves for the first 5 cycles at the scanning rate of  $0.5 \text{ mV s}^{-1}$  are shown in Fig. 5(a). In the first scanning cycle, one characteristic cathodic peak appear at about 0.3 V, indicating the reduction of  $\text{Ni}^{2+}$  to Ni, associating with lithiation reaction to form  $\text{Li}_2\text{O}$  and a partially irreversible solid electrolyte interphase (SEI) film formation. In the subsequent cycles, the cathodic peak potentials shift to 1.0 V and becomes smaller, indicating that an irreversible reaction

present in the first cycle. Two anodic peaks are present around 1.6 and 2.2 V during the charge cycle, corresponding to the decomposition of electrolyte and  $\text{Li}_2\text{O}$  accompanying with the oxidation of Ni.<sup>8, 9, 12, 13</sup> The redox reaction of lithium ions with NiO microspheres electrode can be summarized as follows:

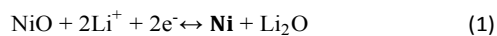


Fig. 5 (b) presents the galvanostatic discharge–charge (GDC) voltage profiles of the porous nanosheets-assembled NiO microspheres carried out at a current density of  $100 \text{ mA g}^{-1}$  for 100 cycles. A long voltage plateau is observed at about 0.65 V, which is due to the reduction of  $\text{Ni}^{2+}$  to Ni and the formation of SEI film. The subsequent GDC cycles demonstrate slow sloped profiles, with plateaus at around 2.2 V upon charge, primarily corresponding to the reversible electrochemical processes of  $\text{Li}_2\text{O}$ . These GDC results are well consistent with the CV results. The initial discharge and charge specific capacities are  $1242 \text{ mA h g}^{-1}$  and  $850 \text{ mA h g}^{-1}$ , respectively, leading to a relatively high coulombic efficiency (CE) of 68 %. The initial capacity loss could be reasonably attributed to the SEI film formation and additional storage of  $\text{Li}^+$  in the pores in the nanosheets or the defects. Moreover, the porous NiO nanosheets are ultrathin so that more crystal facets are exposed to provide additional sites (e.g., more surface defects) for  $\text{Li}^+$  storage.<sup>8, 13, 14</sup>

The NiO microspheres assembled from porous nanosheets also show excellent cycling stability presented in Fig. 5(c). The specific discharge capacity of the NiO microspheres still remains  $820 \text{ mA h g}^{-1}$  at the rate of  $100 \text{ mA g}^{-1}$  after 100 cycles. The result is much better than 3D flower-like NiO hierarchical architectures ( $713 \text{ mA h g}^{-1}$  at  $100 \text{ mA g}^{-1}$  after 40 cycles),<sup>11</sup> and hollow NiO nanotubes ( $726 \text{ mA h g}^{-1}$  at 0.2C after 150 cycles).<sup>21</sup> The coulombic efficiencies keep stable in the scale of 98 – 99%, which increase to almost unity at successive cycles, indicating that the formed SEI film during the first cycle is favorable and stable.<sup>10</sup> Furthermore, the capacity of NiO microspheres increased gradually during the first ten cycles. This is an active process until that the electrolyte completely infiltrates into anode materials, which is usually observed in porous materials. The NiO porous nanosheets can act as a buffer layer to protect the electrode from pulverization due to the volume change and prevent the aggregation of the active materials upon cycling, which is conducive to achieve long term high capacity performance. Furthermore, the 3D microsphere should also be helpful for keeping the structure stability.

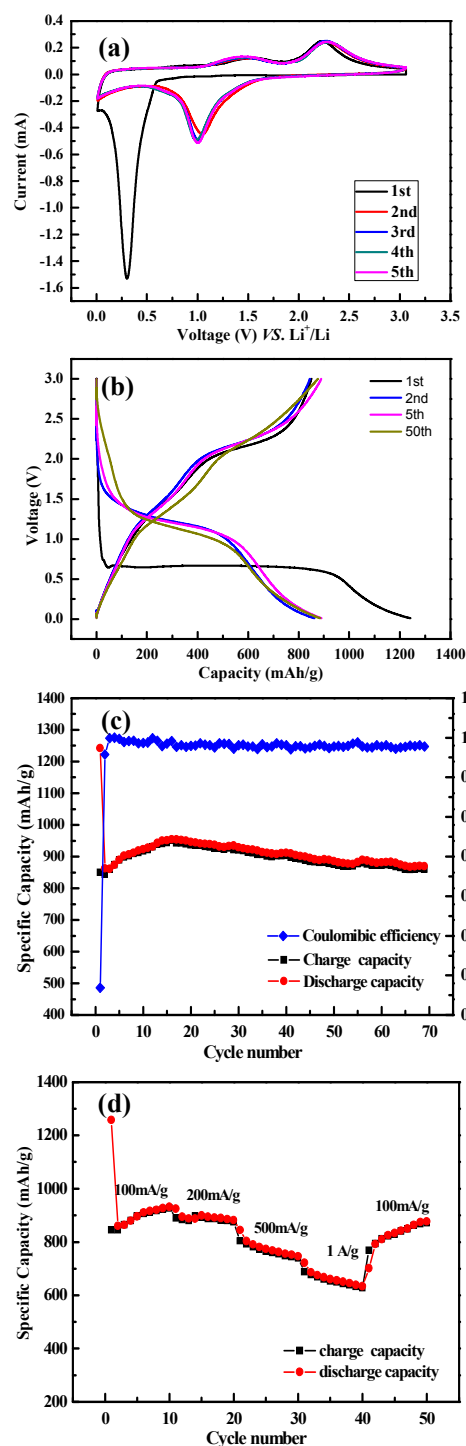


Fig. 5. (a) Representative CVs for the 1<sup>st</sup>, 2<sup>nd</sup>, 3<sup>rd</sup>, 4<sup>th</sup> and 5<sup>th</sup> cycle of the porous nanosheets-assembled NiO microspheres at a scan rate of  $0.5 \text{ mV s}^{-1}$  (b) galvanostatic charge–discharge voltage profiles of the NiO microspheres at a current density of  $100 \text{ mA g}^{-1}$ , (c) comparative cycling performance of the NiO microspheres at a current density of  $100 \text{ mA g}^{-1}$ , and (d) rate performance of the NiO microspheres at different current densities.

Figure 5(d) demonstrates the rate capability of NiO microspheres electrodes from current densities of 100 to 1000 mA g<sup>-1</sup> for ten cycles at each current density. The discharge capacities of NiO microspheres at 100 mA g<sup>-1</sup>, 200 mA g<sup>-1</sup>, 500 mA g<sup>-1</sup>, and 1 A g<sup>-1</sup> are 932 mA h g<sup>-1</sup> (10<sup>th</sup> cycle), 882 mA h g<sup>-1</sup> (20<sup>th</sup> cycle), 746 mA h g<sup>-1</sup> (30<sup>th</sup> cycle) and 634 mA h g<sup>-1</sup> (40<sup>th</sup> cycle), respectively, demonstrating an excellent rate performance for high power lithium ion battery. When the testing current is regularly returned back to low current rate of 100 mA g<sup>-1</sup>, the discharge capacities are recovered to the same level compared to the previous cycles which are running at the same currents. The improved rate performance of the NiO microspheres could also be attributed to ultrathin porous NiO nanosheets. The porous nanosheets can provide sufficient electrode/electrolyte contact areas so that it could supply more reaction sites for lithium ions intercalation/de-intercalation. Moreover, the pores are uniform in size and shape, which is favorable for shortening the Li<sup>+</sup> conducting pathways for rapid charge transfer during the lithiation/delithiation process.<sup>8, 9, 12</sup>

It is worth noting that the NiO microspheres assembled from porous nanosheets show much higher lithium storage capacity, cycle stability and rate performance than other reported NiO nanostructures,<sup>6, 15, 16</sup> demonstrating the advantage and high potential of porous nanosheets assembled NiO microspheres use as anode for LIBs.

In order to understand the superior electrochemical performance of the NiO microspheres assembled from porous nanosheets, EIS measurements were carried out before battery cycling tests and after 100 cycles. The Nyquist plots are shown in Fig. 6. Both profiles exhibit a straight line in the low frequency region, which represents typical Warburg behavior related to the diffusion of lithium ions in the active anode materials.<sup>15, 17</sup> A single depressed semicircle in the high frequency region observed in the impedance spectra of NiO microspheres before cycling is attributed to the impedance of the charge transfer reaction at the interface of electrolyte and active material. However, the Nyquist plots of NiO microspheres after 100 cycles at the delithiation state are composed by two depressed semicircles, one in the high frequency and one in the middle frequency. The cause of the middle frequency semicircle is the same with the one observed in the impedance spectra before cycling. The semicircle observed at the high frequency is due to the formation of the SEI film.<sup>17, 18</sup> Moreover, the charge transfer resistance after 100 cycles is lower than that before cycling, further indicating the existence of active process.

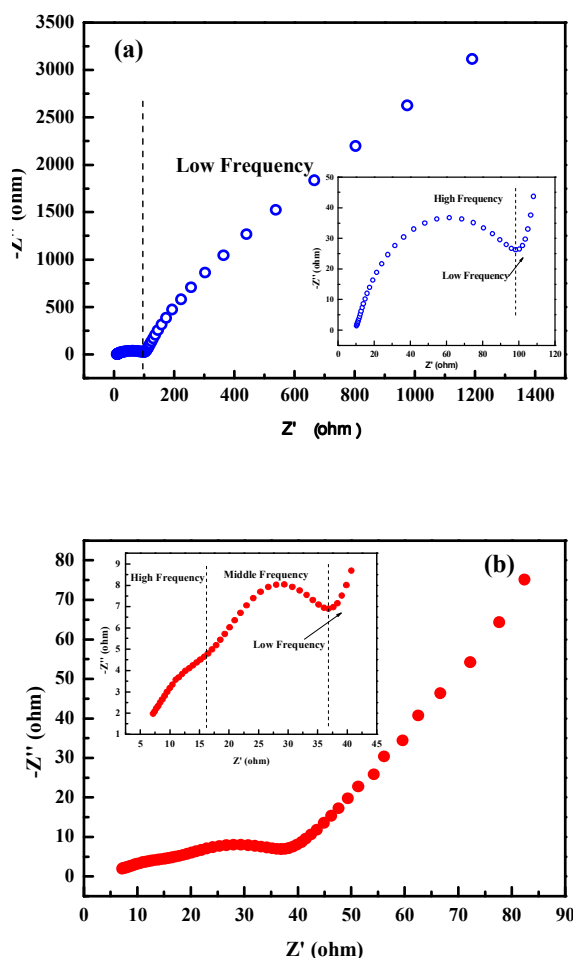


Fig. 6. Electrochemical impedance spectra (100 kHz – 100 mHz) of NiO microspheres: (a) before cycling and (b) after 100 cycles at the delithiation state. Two insets are the corresponding magnified high frequency region of (a) and (b), respectively.

The electrochemical improvement of the as prepared NiO microspheres assembled from porous nanosheets as the anode for lithium ion battery could be reasonably attributed to some desirable advantages related to the unique porous architecture with 3D features. As identified by SEM and BET analysis, the NiO microspheres assembled from the nanosheets with a large amount of pores. The porous nanosheets could buffer the volume change and prevent the aggregation of the active materials upon cycling, which brings about excellent cycling stability. Moreover, the porous nanosheets can provide sufficient electrode/electrolyte contact areas and facilitate the continuous and rapid electron transport through the electrodes. In addition, the 3D microspheres architecture can also helpful for keeping the structure stability of the electrode upon cycling. Thus, the architecture is able to form a stable SEI film quickly and prevent further decomposition of the electrolyte, resulting in the rapid stabilization of columbic efficiencies of 98-99 % and improved rate performance. Furthermore, the porous NiO nanosheets and the SEI film formation contribute most to the

long term high capacity of as prepared NiO microspheres for the lithium ion storage.<sup>9, 13, 19,20</sup> Therefore, the unique 3D architecture assembled from porous nanosheets leads to the anode material for lithium ion battery with high capacity, satisfactory cycle stability and rate performance. Such the 3D NiO microsphere assembled from the porous nanosheets is a promising anode material for high performance LIBs.

## Conclusions

In summary, the NiO microspheres assembled from porous nanosheets were fabricated and exhibited excellent electrochemical performance with a reversible discharge capacity up to 820 mA h g<sup>-1</sup> after 100 cycles at a current of 100 mA g<sup>-1</sup> and ameliorative rate capacity with 634 mA h g<sup>-1</sup> at the current of 1 A g<sup>-1</sup>. These improved and desirable electrochemical performances of the 3D microspheres are primarily attributed to the unique 3D architecture composed of porous nanosheets. The obtained good performance opens up new opportunities in the development of high performance LIBs used for alternative energy and electric transportation.

## Acknowledgements

This work is supported partially by National High-tech R&D Program of China (863 Program, No. 2015AA034601), National Natural Science Foundation of China (Grant nos. 91333122, 51402106, 51372082, and 51202067), Ph.D. Programs Foundation of Ministry of Education of China (Grant nos. 20110036110006, 20120036120006, 20130036110012), Par-Eu Scholars Program, and the Fundamental Research Funds for the Central Universities.

## References

- L. Hu, Z. Tang and Z. Zhang, *Journal of power sources*, 2007, **166**, 226.
- L. Hu, R. Ma, T. C. Ozawa and T. Sasaki, *Angewandte Chemie*, 2009, **121**, 3904.
- L. Hu, R. Ma, T. C. Ozawa and T. Sasaki, *Inorganic chemistry*, 2010, **49**, 2960.
- L. Zhang, H. B. Wu and X. W. (D.) Lou, *Adv. Energy Mater.*, 2014, **4**, 1300958.
- B. Rangasamy, J. Y. Hwang and W. Choi, *Carbon*, 2014, **77**, 1065-1072.
- Y. Chen, B. Song, M. Li, L. Lu and J. Xue, *Adv. Funct. Mater.*, 2014, **24**, 319-326.
- D. S. Guan, J. Y. Li, X. F. Gao and C. Yuan, *RSC Adv.*, 2014, **4**, 4055-4062.
- H. Liu, G. X. Wang, J. Liu, S. Z. Qiao and H. Ahn, *J. Mater. Chem. Phys.*, 2011, **21**, 3046-3052.
- D. Xie, W. W. Yuan, Z. M. Dong, Q. M. Su, J. Zhang and G. H. Du, *Electrochim. Acta*, 2013, **92**, 87-92.
- Y. Huang, X. L. Huang, J. S. Lian, D. Xu, L. M. Wang and X. B. Zhang, *J. Mater. Chem.*, 2012, **22**, 2844.
- Q. Li, Y. J. Chen, T. Yang, D. N. Lei, G. H. Zhang, L. Mei, L. B. Chen, Q. H. Li and T. H. Wang, *Electrochim. Acta*, 2013, **90**, 80-89.
- F. Cao, G. X. Pan, X. H. Xia, P. S. Tang and H. F. Chen, *J. Power Sources*, 2014, **264**, 161-167.
- W. Li, F. Wang, Y. P. Liu, J. X. Wang, J. P. Yang, L. J. Zhang, A. A. Elzatahry, D. Al-Dahyan, Y. Y. Xia and D. Y. Zhao, *Nano Lett.*, 2015, **15**, 2186-2193.
- L. Y. Shen, Z. X. Wang and L. Q. Chen, *RSC Adv.*, 2014, **4**, 15314.
- Y. F. Cui, C. Wang, S. J. Wu, G. Liu, F. F. Zhang and T. M. Wang, *CrystEngComm*, 2011, **13**, 4930.
- D. Xie, Q. M. Su, W. W. Yuan, Z. M. Dong, J. Zhang and G. H. Du, *J. Phys. Chem. C*, 2013, **117**, 24121-24128.
- H. Wang, L. Y. Shi, T. T. Yan, J. P. Zhang, Q. D. Zhong and D. S. Zhang, *J. Mater. Chem. A*, 2014, **2**, 4739.
- F. Jiao, A. H. Hill, A. Harrison, A. Berko, A. V. Chadwick and P. G. Bruce, *J. Am. Chem. Soc.*, 2008, **130**, 5262-5266.
- L. Q. Tao, J. T. Zai, K. X. Wang, Y. H. Wan, H. J. Zhang, C. Yu, Y. L. Xiao and X. F. Qian, *RSC Adv.*, 2012, **2**, 3410.
- J. S. Gnanaraj, E. Zinigrad, L. Asraf, M. Sprecher, H. E. Gottlieb, W. Geissler, M. Schmidt and D. Aurbach, *Electrochem. Commun.*, 2003, **5**, 946-951.
- X. Y. Yan, X. L. Tong, J. Wang, C. W. Gong, M. G. Zhang and L. P. Liang, *Mater. Lett.*, 2014, **136**, 74-77.
- G. M. Zhou, D. W. Wang, L. C. Yin, N. Li, F. Li and H. M. Cheng, *ACS Nano*, 2012, **6** 3214-3223.
- J. C. Guo, A. Sun, X. L. Chen, C. S. Wang and A. Manivannan, *Electrochim. Acta*, 2011, **56**, 3981-3987.
- M. Q. Fan, B. Ren, L. Yu, Q. Liu, J. Wang, D. L. Song, J. Y. Liu, X. Y. Jing and L. H. Liu, *CrystEngComm*, 2014, **16**, 10389-10394.
- X. D. Li, W. Li, M. C. Li, P. Cui, D. H. Chen, T. Gengenbach, L. H. Chu, H. Y. Liu and G. S. Song, *J. Mater. Chem. A*, 2015, **3**, 2762-2769.

**Textual Abstract:**

3D NiO microspheres assembled from porous nanosheets are prepared and evaluated as anode material for lithium ion battery, showing excellent electrochemical performance with high lithium storage capacity, satisfactory cyclability and rate performance. The NiO microspheres deliver a first discharge capacity of  $1242 \text{ mA h g}^{-1}$  and remain a reversible capacity up to  $820 \text{ mA h g}^{-1}$  after 100 cycles at a current of  $100 \text{ mA g}^{-1}$  in half cell. And it exhibits ameliorative rate capacity of  $634 \text{ mA h g}^{-1}$  at the current of  $1 \text{ A g}^{-1}$ . The high lithium-storage performance can be mainly ascribed to the porous nanosheets, which improve lithium ions transfer, provide sufficient electrode/electrolyte contact areas and better accommodation of volume change with the lithiation/delithiation process. Moreover, the 3D microsphere architecture are also helpful for enhancing the electrochemical performance of the lithium ion battery. The results indicate the great potential of the 3D NiO microspheres assembled from porous nanosheets used as the anode materials for lithium ion batteries.

**Graphical Abstract:**